

## The Response of Temperature and Velocity Fields to $M_2$ Tide in Deukryang Bay in the Southern Sea of Korea

Chul-hoon HONG and Yong-Kyu CHOI\*

*Pukyong National University, Pusan 608-737, Korea*

*\*Kunsan Laboratory West Sea Fisheries Research Institute,*

*National Fisheries Research and Development Agency, Kunsan 573-030, Korea*

A primitive equation numerical model driven only by  $M_2$  tide is used to examine role of tide in the temperature and velocity fields of Deukryang Bay. The numerical model reproduces several features of the observational temperature fields such that the isotherms tend to be parallel to the coast in the bay, and the colder water exists at the right hand side in the bay. The horizontal temperature and velocity fields in the model are dominantly influenced by bottom topography. The model also shows that the surface colder water in the bay is accompanied by strong-alongshore current during the flood tide. An investigation for baroclinicity in the bay by additional numerical experiment indicates that the baroclinicity in velocity field is very weak. The model, however, did not reproduce a stratification in the observation, implying that the model needs to add other semi-diurnal components such as  $S_2$ ,  $O_2$  or  $K_2$  tides to  $M_2$  tide.

**Key words :**  $M_2$  tide, bottom topography, baroclinicity, stratification semi-diurnal components

### Introduction

Circulation in a small bay around coastal area is basically controlled by tidal motion so that it is predominantly barotropic. However, the cause of temperature distribution in the bay, such as Deukryang Bay which is located at southern coast of Korea (Fig. 1) is subject to debate relating to biological phenomena. The response of the bay to tidal forcing,  $M_2$  tide including a temperature field is the focus of this paper.

Temperature distribution of Deukryang Bay in summer in 1994 is given in Fig. 2 (after Choi et al., 1995). We can find some interesting features, i.e. the isotherms tend to be parallel to the coast in the bay, and colder water exists at the right hand side of the bay. In particular, surface water in the spring tide (Fig. 2a) is colder with about 2~3°C than that in the neap tide (Fig. 2b). The vertical profiles of temperature along line C in 1992-1994 (Fig. 3) shows a relationship between stratification and tide. The stratification in the spring tide is significantly weaker than that in the neap tide, as indicated by Lee (1994). These observations illustrate tidal effect in the temperature field of Deukryang Bay. From above results we are interested in investigating an effect of tide on temperature field using a three dimensional numerical model.

Numerical studies of circulation in Deukryang Bay

first were carried out by Yosu Nat's University (1992) within a small area of the bay to investigate an effect of damage due to a construction, and Jung et al. (1994) extended the calculation to all area of the bay using a shallow water model. Tidal currents calculated by Jung et al. (1994), which is forced by  $M_2$  tide, are given in Fig. 4. In general the current is stronger in the right hand side of the bay and flows along the coast as indicated by them (also they showed that the model velocity corresponds well to the observations in their figures' 2 and 3, not presented here). However, they could not give a vertical structure of velocity field as well as a temperature field in the model due to an inherent limitation of their models. To examine the role of tide in a temperature field of the bay, we utilize a primitive equation model described in detail by Blumberg and Mellor (1987). This model are well documented and reproduce many of the observed features of the coastal and estuarine water (Hukuda et al., 1994; Galperin and Mellor 1990 a, b; Oey et al., 1985), and large scale circulations (Zavatarelli and Mellor, 1996; Mellor and Ezer, 1991). The model is driven only by  $M_2$  tide of semi-diurnal components of tide which occupy about 90 % of total energy in Deukryang Bay (Lee et al., 1995).

In the next section, a discussion of the model is presented. The following section presents temperature and velocity fields of the model in the bay, and also presents

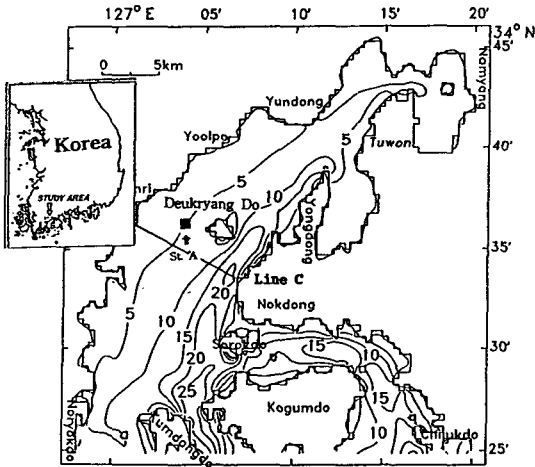


Fig. 1. The model bottom topography of Deukryang Bay. Depths are in meters. St. A represents a velocity observation point. The observed vertical temperature distribution is shown on Line C.

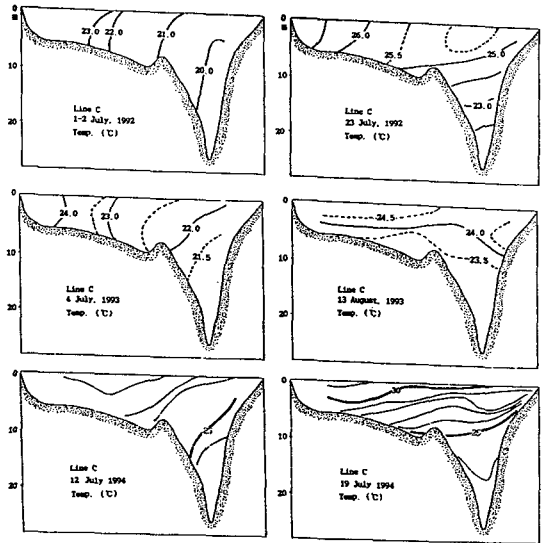


Fig. 3. The vertical profiles of temperature on line C in 1992~1994.

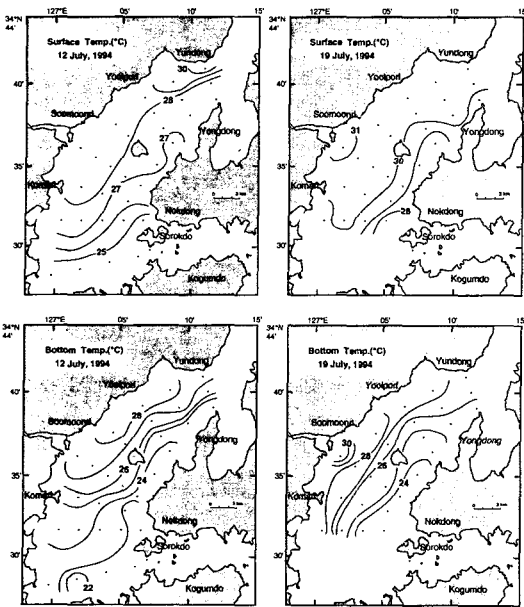


Fig. 2. The temperature distribution of Deukryang Bay at surface (upper panel) and bottom layer (lower panel) in the spring tide (a) and neap tide (b) in summer, 1994 (Choi et al., 1995).

a study of bottom topographic effect. The conclusions follow.

Numerical Model

The model is the Princeton ocean model (Blumberg and Mellor, 1987). It is a primitive equation model with a free surface, a split mode time step, and solves the following equations, i.e. continuity, momentum, hydrostatic, temperature, salinity and density equations which are given by

$$\frac{\partial u}{\partial x} + \frac{\partial v}{\partial y} + \frac{\partial w}{\partial z} = 0 \tag{1}$$

$$\frac{\partial u}{\partial t} + u \frac{\partial u}{\partial x} + v \frac{\partial u}{\partial y} + w \frac{\partial u}{\partial z} - f v = -\rho_0^{-1} \frac{\partial p}{\partial x} + \frac{\partial}{\partial z} (K_M \frac{\partial u}{\partial z}) + F^x \tag{2}$$

$$\frac{\partial v}{\partial t} + u \frac{\partial v}{\partial x} + v \frac{\partial v}{\partial y} + w \frac{\partial v}{\partial z} - f u = -\rho_0^{-1} \frac{\partial p}{\partial y} + \frac{\partial}{\partial z} (K_M \frac{\partial v}{\partial z}) + F^y \tag{3}$$

$$\rho g = -\frac{\partial p}{\partial z} \tag{4}$$

$$\frac{\partial T}{\partial t} + u \frac{\partial T}{\partial x} + v \frac{\partial T}{\partial y} + w \frac{\partial T}{\partial z} = \frac{\partial}{\partial z} (K_H \frac{\partial T}{\partial z}) + F^T \tag{5}$$

$$\frac{\partial S}{\partial t} + u \frac{\partial S}{\partial x} + v \frac{\partial S}{\partial y} + w \frac{\partial S}{\partial z} = \frac{\partial}{\partial z} (K_H \frac{\partial S}{\partial z}) + F^S \tag{6}$$

$$\rho = \rho(T, S) \tag{7}$$

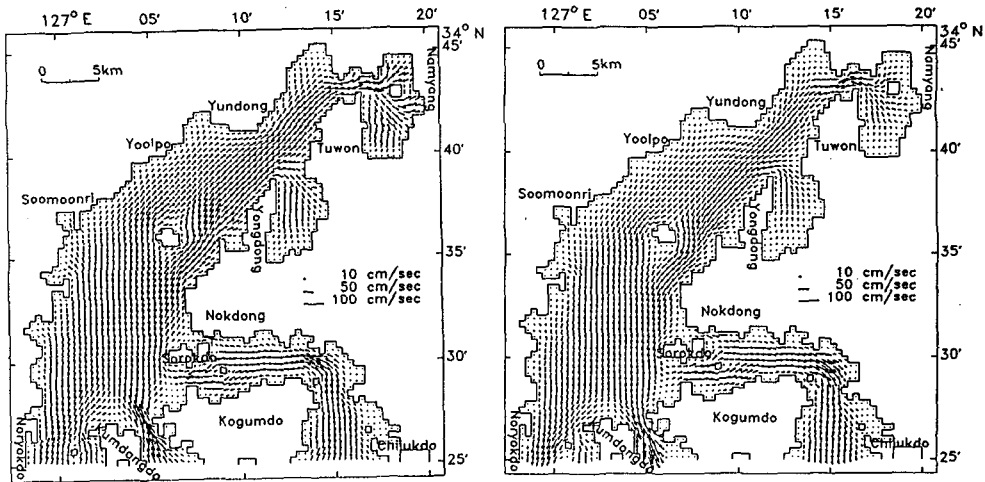


Fig. 4. Tidal current in Deukryang Bay in the flood tide (a) and the ebb tide (b) (after Jung et al., 1994)

where  $u, v, w$  are the velocity components in the  $x, y, z$  directions, respectively,  $p$  the pressure,  $T$  the temperature,  $S$  the salinity,  $\rho$  in situ density,  $\rho_0$  (= constant) the reference density,  $f$  the Coriolis parameter,  $g$  the gravity,  $K_H$  the vertical eddy viscosity,  $K_M$  the vertical eddy diffusivity,  $F^{(T,S)}$  the horizontal eddy friction terms, and  $F^{(T,S)}$  the horizontal eddy diffusion terms. The model assumes the Boussinesq and hydrostatic approximations, and uses the Knudsen's equation for solving the equation (7). The  $K_M, K_H$  are determined by Mellor and Yamada level 2.5 turbulence closure model (Galperin et al., 1988). The horizontal friction and diffusion terms are given by the Laplacian forms with the coefficients  $A_M$  and  $A_H$  given by Smagorinsky nonlinear viscosity. The model is first reconstructed (1)~(6) on  $\sigma$ -coordinate system defined by  $\sigma = (z - \eta) / (H + \eta)$  where  $\eta$  and  $H$  are the surface elevation and the water depth, respectively. In that transforms the horizontal friction and diffusion terms are treated according to Mellor and Blumberg (1985) who argued that the horizontal diffusion takes place along the constant  $\sigma$  levels. Asselin filtering method is used every time step to prevent a split in the solution associated with the leapfrog scheme. A more detailed description of numerical schemes is given by Blumberg and Mellor (1987).

Topography of Deukryang Bay to which we apply the model is depicted in Fig. 1 as an idealized form. Note that the zonal topography is very steep at the right hand side in the bay, and the isobaths tend to be parallel to

the coast. Circulation in the bay may be significantly controlled by the topographic effect. This will be discussed in next section. At the first stage of the present study the model is driven only by  $M_2$  tide.

The normal components of velocity at coastal boundary are chosen to be zero. At open boundary the normal components of the external mode velocity ( $\bar{v}_b$ ) is calculated from a linearized momentum equation. In this process horizontal friction terms are included to avoid an instability within the first tidal period (Hukuda et al., 1994). For the internal mode velocity ( $v_b$ ) a radiation condition of Orlanski (1976) is given. The tangential components of both external and internal mode velocities are subject to free slip condition,  $\partial \bar{u} / \partial y = \partial u / \partial y = 0$ . The same condition is also given for temperature and salinity. Initial temperature condition is horizontally homogeneous with vertical structure similar to that observed in Deukryang Bay (Kim, 1993) as shown in Fig. 5. A thermocline is present at 5~15 m depth. Salinity distribution, on the other hand, is assumed to be equal everywhere to 34.5 ‰ and used as a check on the conservation properties of the finite difference technique. Initial sea level and velocities are set to be zero,  $u = v = \eta = 0$ . Wind and river discharges are not involved in the model, and also the heat exchanges are neglected on assumption of few variation of heat flux through surface or open boundaries for run-time of the model.

The horizontal grid is fixed to 1 km in both  $x$  and  $y$  directions. The model consists of 10 vertical levels with

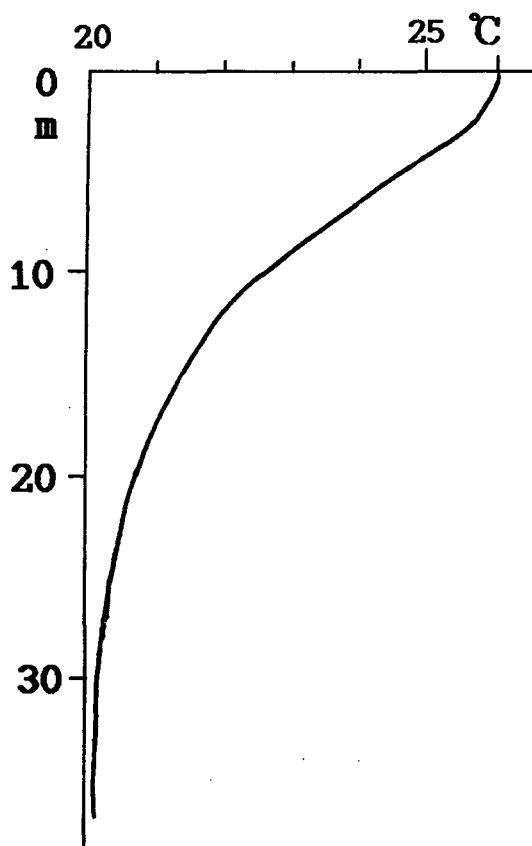


Fig. 5. Initial temperature distribution in the model. The distribution is typical of that observed in Deukryang Bay.

irregular vertical spacing in  $\sigma$  space as listed in Table 1. Note to show a fine resolution in the surface layer. Considering CFL condition, the time steps are set to 10 seconds for the external mode and 100 seconds for the internal mode. Bottom drag coefficient and horizontal drag coefficient (Smagorinsky constant) are set to  $2.5 \times 10^{-3}$  and  $10^{-2}$ , respectively. The model is run for 10 tidal periods (about 5 days) and the results of final 12 hour period are presented. In this run-time tidal motion was almost stable, i.e. implying small baroclinicity (See section 3). Of course, in this period a steady state solution of temperature fields can not be obtained because the water in the condition will be finally homogeneous. However, to some extent a comparison of the model with the observation can be possible because a heat exchange in the bay through boundaries would be assumed to be small in this period. The model results in the

Table 1. Vertical  $\sigma$  coordinate distribution

Level	$\sigma$	$\sigma'$	$\Delta\sigma$
1	0.00		
2	-0.021	-0.010	0.021
3	-0.042	-0.029	0.021
4	-0.083	-0.059	0.042
5	-0.167	-0.118	0.083
6	-0.333	-0.236	0.167
7	-0.500	-0.417	0.167
8	-0.667	-0.583	0.167
9	-0.833	-0.764	0.167
10	-1.000	-0.917	0.167

The quantity  $\sigma$  is depths at which turbulence quantities and the vertical velocity are located,  $\sigma'$  corresponds to the depth at which horizontal velocity, temperature, salinity, and density are defined, and  $\Delta\sigma$  is the grid spacing.

flood and ebb tides are compared with observational results in the spring and neap tides. These comparisons will be possible when  $M_2$  tide is very larger than other tidal components, e.g.  $S_2$ ,  $O_2$  and  $K_2$  tides. The model results, however, give some discrepancies between the model and the observation (temperature field). We will discuss about that in the next section.

## Results

Fig. 6 shows temperature fields of the model at level 3 (upper panels) and level 8 (lower panels). The model reproduces several features of the observational temperature fields as shown in Fig. 2. That is; the isotherms are generally parallel to the coast, and the colder water exists in the right hand side of the bay. Surface water in the flood tide (Fig. 6a) tends to be colder than that in the ebb tide (Fig. 6b), although the difference between them is small with about  $0.5^\circ\text{C}$ , probably associated with initial temperature field, whereas in the lower layer there are few change of horizontal temperature field during

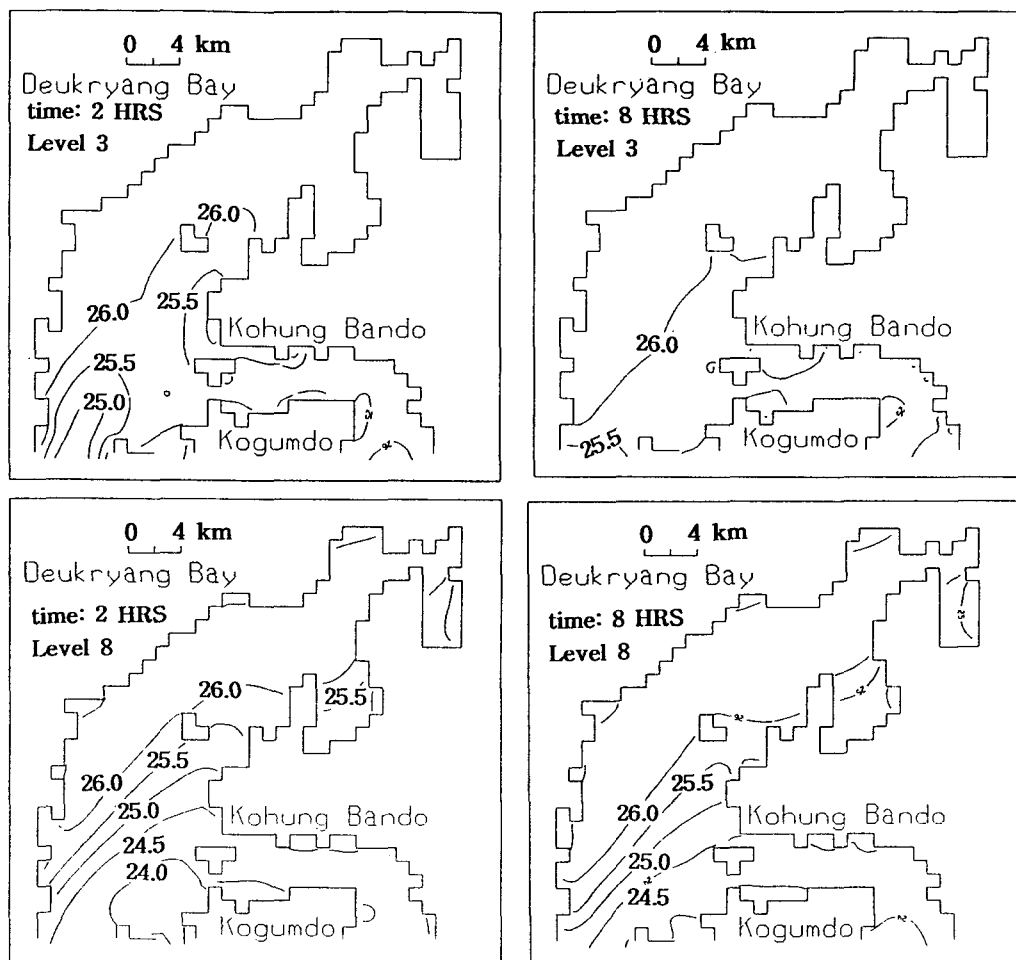


Fig. 6. The temperature fields of the model in the flood (a) and the ebb tide (b).  $CI=0.5^{\circ}C$ .

these periods as the observation (Fig. 2a, 2b; lower panels). Note the surface cold water transported into the bay at the west of Kogumdo in the flood tide (Fig. 6a). Velocity fields at level 3 and level 8 in Fig. 7 show that this cold water is accompanied by the strong-alongshore current in the flood tide. The pattern of the horizontal velocity fields in the bay is basically similar to the results obtained from a shallow water numerical model by Jung et al. (1994) (the mean velocity field in the present model is not presented because of the almost similar to theirs). The velocities in the flood and ebb tides have values between 30 cm/s and 90 cm/s at level 3, and between 10 cm/s and 40 cm/s at level 8. Lee et al. (1995; Fig. 2) presented time series of surface velocity at the upper layer (about 2 m) at St. A in Fig. 1 which gives ranges between about 10 and 50 cm/s in the flood and

ebb tides, as shown in Fig. 8. The model velocity at the same place illustrates values between 20 and 60 cm/s which correspond well to the observation. The velocity fields in the model, as the temperature field (Fig. 6), also have a horizontal contrasts as already shown in Fig. 4 calculated by Jung et al. (1994), i.e. stronger velocity fields exist in the right hand side of the bay. These horizontal contrasts are influenced by bottom topography. This will be discussed later.

In Fig. 9 the vertical section of velocity along line C is given. The existence of vertical velocity shear in the bay for all tidal period clearly is showed, as pointed out from a temporary current measurement by Shin (1993). Main axes of the current are located at the deepest places, and their locations are slightly changed according to tidal period. Especially the velocity values in the ebb

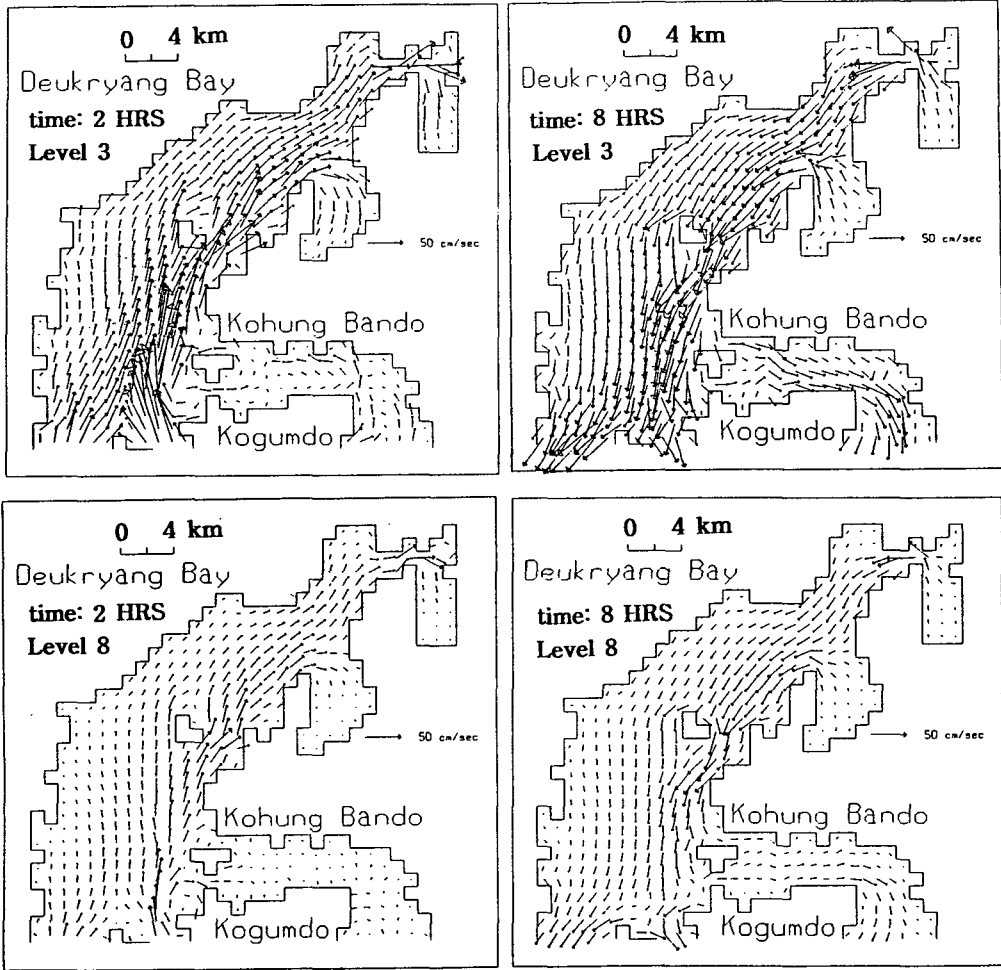


Fig. 7. The internal velocity fields at level 3 and level 8 in the flood (a) and the ebb tide (b).

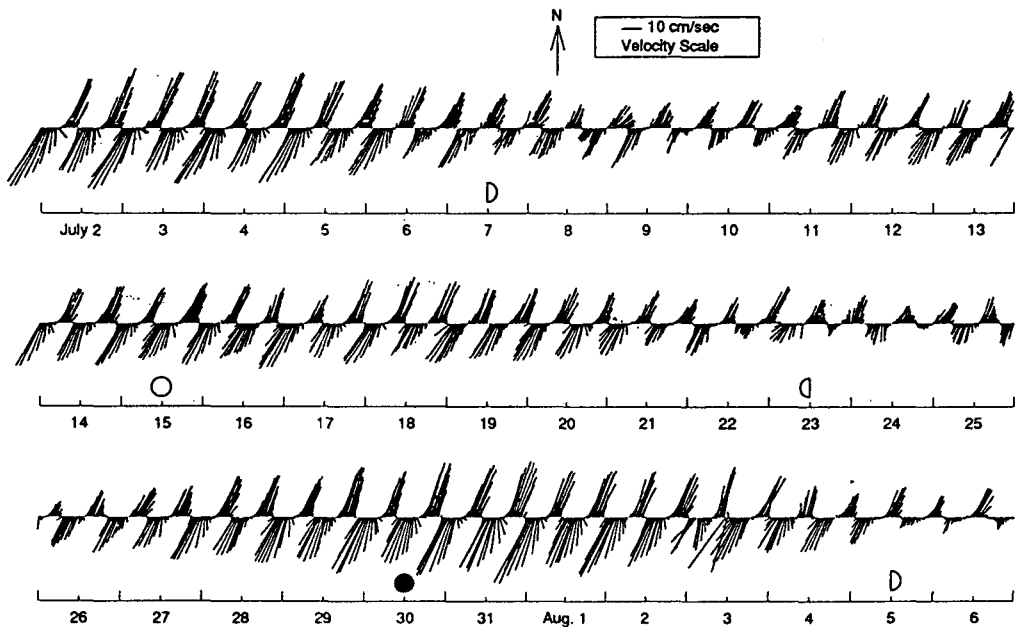


Fig. 8. The time series of velocity at St. A, 1992 (after Lee et al., 1995).

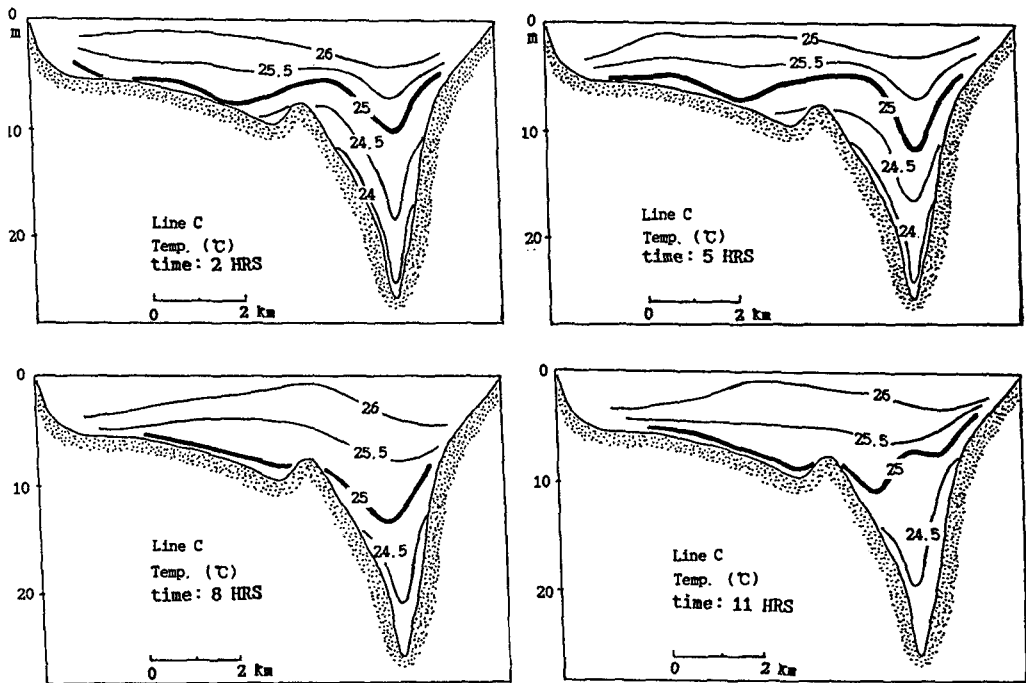


Fig. 9. Alongshore velocity in the model along vertical section on line C.

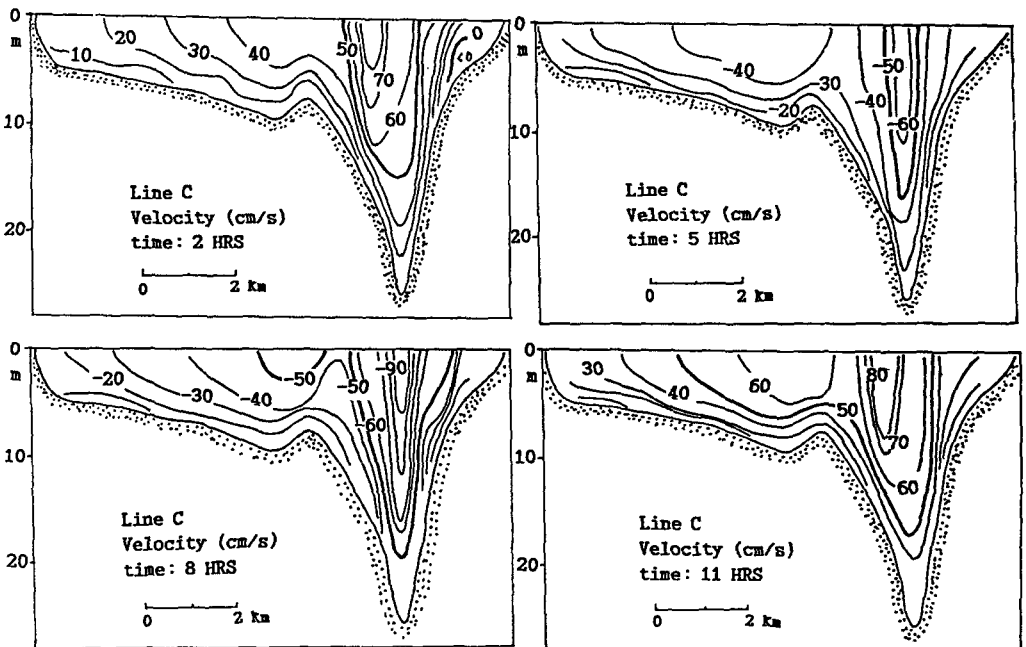


Fig. 10. The vertical section of temperature in the model in the flood (a) and the ebb tides (8b) along line C in Fig. 1.  $Cl=0.5^\circ\text{C}$ .

tide are generally larger (about 10 cm/s) than that in the flood tide. This tendency also corresponds to the observation (Fig. 8). In general, the flow directions at the up-

per and lower layers are similar and imply that the barotropic flow field is dominant.

Fig. 10 gives the calculated temperature along the

line C. Colder water layer depth in the right hand side of the bay is slightly more deepened in the flood tide (2 hrs) than in the ebb tide (8 hrs). This indicates that the cold water at the right hand side of the bay is formed by the inflow as given in Fig. 6 and Fig. 7. The model, however, did not reproduce strong contrasts of stratifications between the flood and ebb tides as given in Fig. 3, because probably it is subject to be forced only by  $M_2$  tide. To reproduce a contrast of stratification in the bay, more detailed numerical study including other tidal components, e.g.  $S_2$ ,  $O_2$  and  $K_2$  will be necessary in the future.

As we already indicated, zonal topography in Deukryang Bay is very steep in the right hand side, and the isobaths tend to be parallel to the coast of the bay. In the model and the observations (Figs. 2, 5, and 6) we ob-

tained the distributions of the isotherms similar to the isobaths. The relationship between the temperature and /or the velocity field, and bottom topography is simply investigated using a flat bottom model with depth of 40 m. All the conditions of the experiment (hereafter, Ex 2) are the same as the basic experiment (hereafter, Ex 1) except for the constant depth.

Fig. 11 gives temperature fields in the flood (Fig. 11a) and the ebb tides (Fig. 11b) in Ex 2. Note that the horizontal contrasts as shown in Fig. 6 (Ex 1) has entirely disappeared in the lower layers (level 8) where tidal current becomes weaker due to bottom friction, while they still remains around entrance of the bay in the upper layer (level 3). Velocity fields in Ex 2 in Fig. 12 show the same tendency as the temperature fields. Consequently, these results show that the distributions of

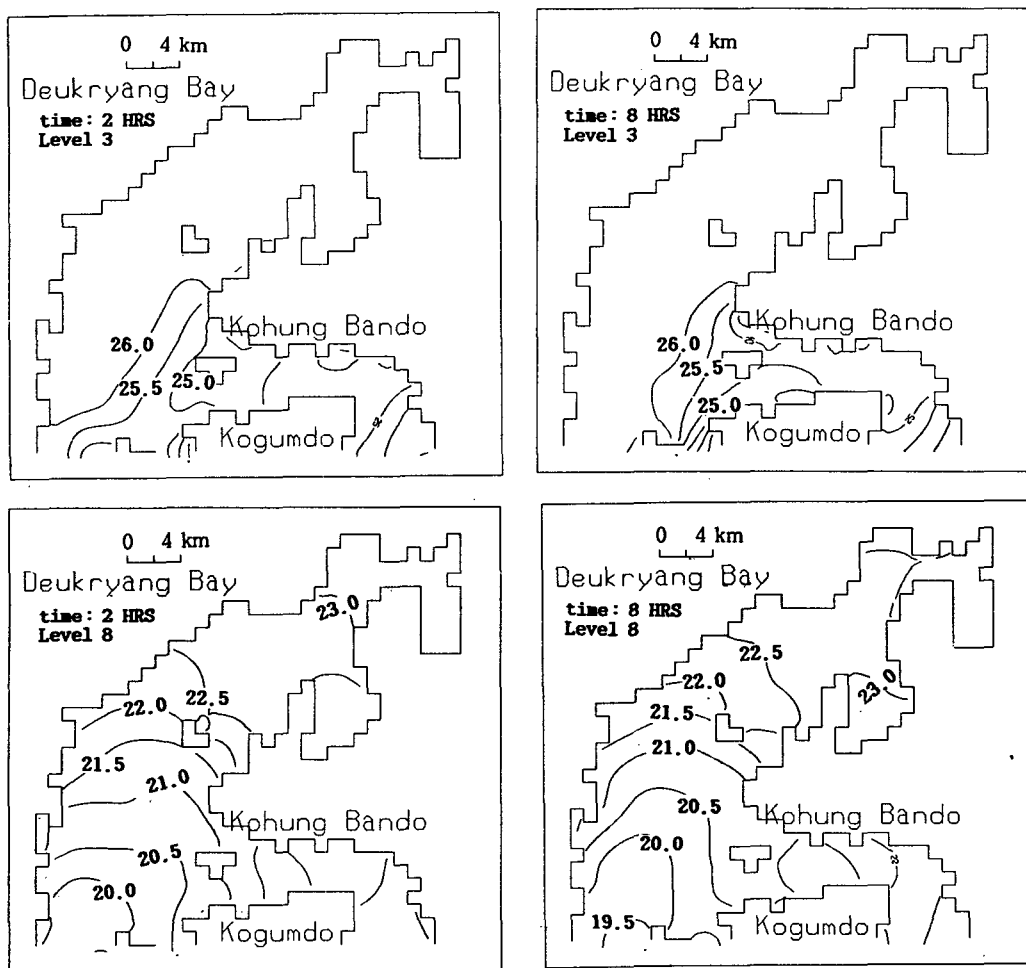


Fig. 11. The temperature fields in the flood (a) and the ebb tides (b) in Ex. 2.  $CI=0.5^{\circ}\text{C}$ .



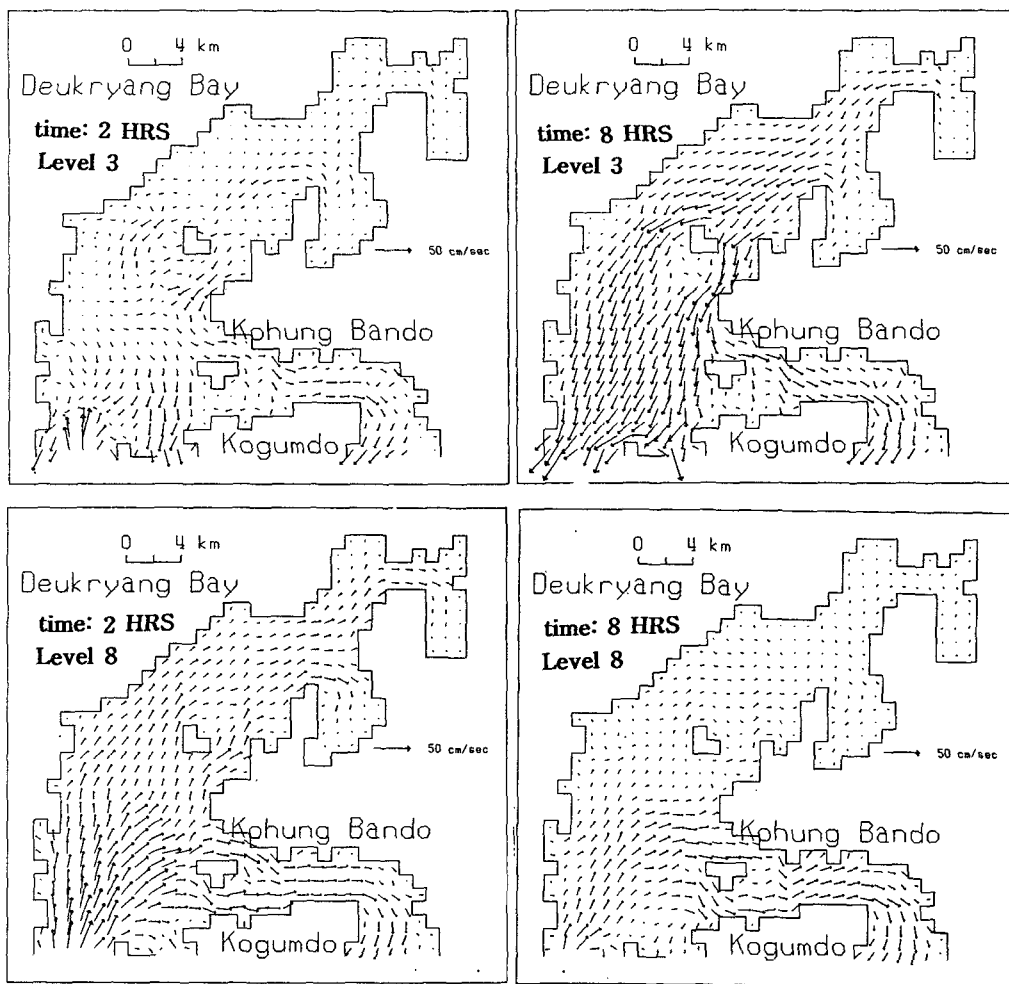


Fig. 12. The velocity field in the flood (a) and the ebb tides (b) in Ex. 2.

temperature and velocity fields in the bay have been influenced by the bottom topography, especially in the lower layers. This implies that tidal effect in the surface layer seems to be more dominant than the topographic effect. Velocity directions between the upper and lower layers (Fig. 12) are opposite each other due to dominant role of internal waves.

Finally, to see how baroclinicity modifies velocity field in the bay, we run a shallow water model of which all conditions are the same as Ex 1 except for elimination of baroclinicity. The present model (Blumberg and Mellor, 1987) is optionally possible to examine a barotrophy. Each mean flow field averaged over 12 hours period are given in Fig. 13 (Note enlarged arrows of velocity vectors). The velocity field in Ex 1 (Fig. 13a) including a

baroclinicity is intensified about 30~50% (3~5 cm/s) than that in the homogeneous model (Fig. 13b) especially around the bay entrance or Deukryang Do which are deeper places in the bay (Fig. 1). This shows that baroclinicity in the flow field in the bay is very weak.

### Conclusions and Discussion

A primitive equation numerical model driven only by  $M_2$  is used to examine role of tide in temperature and velocity fields of Deukryang Bay. The results of numerical experiments represent several features of the observational temperature and velocity fields, such as reproducing horizontal distributions or contrasts of temperature. The model shows that horizontal temperature

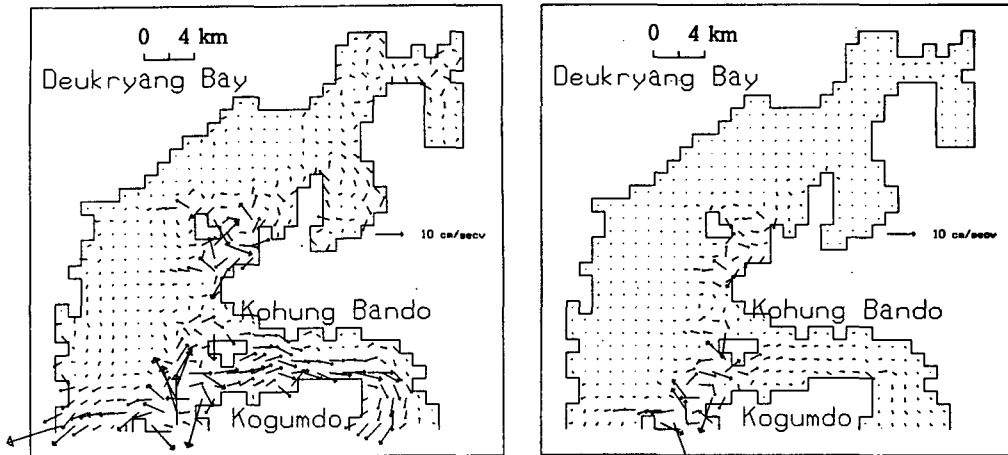


Fig. 13. The mean current vectors averaged over 12 hour period in Baroclinic model (a) and homogeneous model (b). Note that arrow scale is enlarged compared with Fig. 7.

and velocity fields are dominantly influenced by bottom topography of which the effect makes the velocity field in the right hand side of the bay more stronger. The model also shows that surface colder water in the bay is accompanied by a strong-alongshore current during the flood tide. Vertical velocity shear exists. An experiment to examine baroclinicity in the velocity field indicates that it is very weaker than barotropy in the velocity field. Hukuda et al. (1994) reported that baroclinic velocity field can be modified by runoff from a large river. In Deukryang Bay there is a few river such as Soomoonli stream of which runoff seems to be small. However, if we can take into account such runoff into the bay, the velocity or density field might be slightly modified. The horizontal space resolution in the model was coarse with  $1\text{ km} \times 1\text{ km}$ . If we adopt fine resolution the flow field near to eastern boundary with horizontally steep topography may be partly modified. Our model was not considered variation of salinity, wind effect, or heat flux at open boundaries. Also the model could not give a good steady solution due to a simple boundary condition. Especially the model did not reproduce strong stratification similar to the observation. Probably this will be related to consider only  $M_2$  tide as a forcing. In next study we will consider the effect of other semi-diurnal tidal components, e.g.  $S_2$ ,  $O_2$  and  $K_2$ . In summary, although we could not fully reproduce the temperature and velocity fields in the bay due to various problems discussed above, the model was partially successful, and the study for the improvement of

a model performance will be conducted experimentally and theoretically in the future.

### Acknowledgement

The author thanks Dr. H. Hukuda for helping the modelling establishment, and Prof. J.H. Yoon for useful comments. We are very grateful to the editor and to the two anonymous reviewers for carefully reading the manuscript and for giving many comments. This study was supported in part by the Korea Science and Engineering Foundation (KOSEF) through the Research Center for Ocean Industrial Development (RCOID) of Pukyong National University in 1995.

### References

- Blumberg, A.F. and G.L. Mellor. 1987. A description of a three dimensional coastal ocean circulation model. In *Three Dimensional Coastal Ocean Models*, Coastal Estuarine Science, 4th, ed. by N.S. Heaps, American Geophysical Union, Washington D.C., 1~16.
- Cho, Y.K., B.G., Lee, K.D., Cho and C.H., Hong. 1995. Environmental variations of culturing ground of penshell (*atrina pectinata*) according to the depth at Deukryang Bay. *Bull. Korea Soc. Fish. Tech.* 31, 127~141 (in Korean).
- Galperin, B., L.H. Kantha, S. Hassid and A. Rosati. 1988. A quasi-equilibrium turbulent energy model for geophysical flows. *J. Atmos. Science*, 45, 55~62.

- Galperin, B., and G. L. Mellor. 1990a. A time-dependent, three-dimensional model of the Delaware Bay and River. Part 1. Description of the model and tidal analysis. *Estuarine Coastal Shelf Sci.*, 31, 231~253.
- Galperin, B., and G. L. Mellor. 1990b. A time-dependent, three-dimensional model of the Delaware Bay and River. Part 2. Three dimensional flow fields and residual circulation. *Estuarine Coastal Shelf Sci.*, 31, 255~281.
- Hong S.Y., C.W. Ma and H.S. Lim. 1995. Macrobenthic fauna of the Deukryang Bay. *Bull. Korea Fish. Soc.* (in Korean). (submitted) Hukuda H., J.H. Yoon and T. Yamagata. 1994. A tidal simulation of Ariake Bay-A tideland model. *J. Oceanogr. Soc. Japan*, 50, 141~163.
- Jung E.J., C.H. Hong, B.G. Lee and K.D. Cho. 1994. A numerical study on the circulation in Deukryang Bay. I. Tidal circulation forced by  $M_2$  tide. *Bull. Korea Fish. Soc.* 27, 397~403 (in Korean).
- Kim, S.U. 1993. The study of oceanographic characteristics in Deukryang Bay, in 1992-1993. M.S. Thesis, Nat'l Fish. Univ. Pusan. 47 pp. (in Korean).
- Kong Y.S. and B.G. Lee. 1994. Surface sediment and suspended material in Deukryang Bay. *J. Kor. Soc. Oceanogr.* 29, 269~277 (in Korean).
- Lee, B.G. 1994. A study of physical oceanographic characteristics of Deukryang Bay using numerical and analytical model in summer. Ph.D. Thesis, Nat'l Fish. Univ. Pusan. 145 pp.
- Lee, J.C., H.K. Rho, K.D. Cho, S.W. Shin, and S.H. Kim. 1995. Tidal current in the Weatern Part of Deukryang Bay in Summer 1992. *Bull. Korea Fish. Soc.* 28 : 1~6. (in Korean).
- Mellor, G.L. and A.F. Blumberg. 1985. Modeling vertical and horizontal diffusivities with the sigma coordinate system. *Mon. Wea. Rev.*, 113, 1379~1383.
- Mellor, G.L., and T. Ezer, 1991. A Gulf stream model and an altimetry assimilation scheme. *J. Geophys. Res.*, 96, 8779~8795.
- Oey, L. Y., G. L. Mellor, and R. I. Hires. 1985. A three-dimensional simulation of the Hudson Raritan estuary. Part I. Description of the model and model simulations. *J. Phys. Oceanogr.*, 15, 1676~1692.
- Orlanski, I. 1976. A simple boundary condition for unbounded hyperbolic flows. *J. Comput. Phys.*, 21, 251~269.
- Shin, S.I. 1993. The oceanic condition and tidal characteristics in Deukryang Bay. M.S. Thesis, Nat'l Fish. Univ. Pusan. 41pp. (in Korean).
- Zavaterelli, M., and G. L. Mellor. 1995. A numerical study of the Mediterranean Sea circulation. *J. Phys. Oceanogr.*, 25, 1384~1414.

---

Received January 10, 1995

Accepted July 5, 1997

## 특량만에서의 $M_2$ 조에 대한 수온장 및 유속장의 응답

홍철훈 · 최용규\*

부산수산대학교 해양산업개발연구소, \*수산진흥원 서해수산연구소

$M_2$  조에 의해 구동되는 원시방정식을 이용한 수치모델이 특량만에서 수온장 및 유속장에 미치는 조석의 효과를 조사하기 위해 이용된다. 모델결과는 관측된 수온장의 여러 가지 특징을 재현하였다. 즉 등온선이 만내의 연안선과 평행한 점, 냉수가 만의 우측에 나타나는 점 등이었다. 특히 실험결과로 볼 때 수평 수온장 및 유속장은 해저지형효과를 크게 받고 있으며 만내의 표층냉수는 고저시의 유입되는 흐름에 수반된다. 경압성을 조사하기 위한 추가적인 수치실험결과는 유속장내의 경압성이 매우 약함을 보여준다. 그러나 실험결과는 관측에서 보여준 밀도성층구조를 재현하지 못했다. 이를 재현하기 위해서는  $M_2$  조 이외에  $S_2$ ,  $O_2$  또는  $K_2$  조를 외력에 포함시켜야 할 것으로 예상된다.